PENDULUM WITH HOOP-TYPE FLOW ENERGY CONVERTER SYSTEM

Yutaka Terao
Tokai University, Shizuoka, Japan

A new hoop-type energy conversion system installed in a pendulum-type device is proposed and tested. The rolling cylinder is used VIM phenomena and rotating hoop comprise the double pendulum system and these systems exhibit chaos in some cases. An equation of pendulum–hoop motion was developed to provide numerical solutions when the onset of chaos occurs.

Keywords: Hoop generator, Vortex-induced motion (VIM), Chaos, Flow energy harvesting

1. INTRODUCTION

Energy harvesting is an important and necessary process for determining how to utilize natural energy resources. This paper discusses a new energy absorption system that takes advantage of flow energy. [The speed of the flow is relatively low but has not yet been fully utilized. The relatively slow flow energy absorption means that the extraction and conversion of energy from thin density energy distribution is difficult. One advanced and elegant energy harvesting device is the VIVACE converter proposed by the University of Michigan in the USA. Using the vortex-induced motion (VIM) of a cylinder, the VIVACE converter has high performance even in a fluid flow, and most importantly, the mechanism of this system is simple. The cylinder in the VIVACE converter produces a large parallel motion and is connected to a generator, and electric power is then generated from the oscillating motion of the cylinder. In contrast, Japanese researchers proposed another device utilizing vortex-induced vibration (VIV), hereafter referred to as the pendulum-type generator. This device consists of a floater cylinder pendulum connected to a pin joint, as shown in Figure 1, and the cylinder moves with a swinging roll motion in the fluid flow. The pendulum-type generator showed higher performance than the VIVACE converter.

This paper discusses a newly developed hoop-type generator system installed on a swinging cylinder, similar to that shown in Fig 2. The purpose of this system is to improve the generating performance of the pendulum-type generator. Our system comprises a double pendulum; one pendulum is an oscillating cylinder, and the other is a hoop with unbalanced mass. In this case, it is expected that the rotational motion of the hoop will be chaotic. Because the large amplitudes of the motions of the hoop angle and pendulum easily cause nonlinear oscillation and a nonlinear restoring force, the gravitational force component may lead to the onset of chaos, which makes describing the system much more complex.
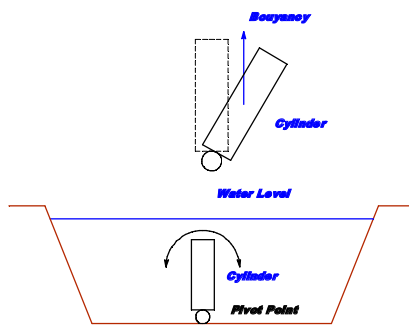
seagull1@scc.u-tokai.ac.jp
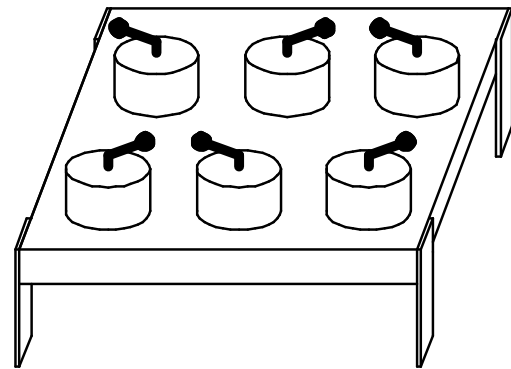
Figure 1. Schematic of pendulum-type generator[1].


Figure 2. Hula-hoop energy absorber[3].

2. WATER TANK TEST

A circular water tank test was conducted with polyvinyl chloride cylinders of a small diameter to confirm the VIM phenomenon. The test setup is shown in Photographs 1 and 2. The cylinder pivot point is set 500 mm under the free surface. The hoop system was set on the top of the cylinder. Four sets of hoop generators and measurement equipment were prepared as shown in Photograph 3. The electric power generated by the hoop generator and the roll angle sensor of the cylinder were included in the devices. Data were obtained via a local area network (LAN) cable. The measured 8-channel (8CH) signal was amplified by operation amplifiers, and the offset was simultaneously adjusted. Photograph 4 shows the newly developed data logger system, which uses the single-chip microcontroller PIC18F2553. A 12-bit analog-to-digital (A/D) converter output an 8CH signal every 20-Hz sampling period, and these output signals were downloaded to a PC through RS-232C communication and a USB converter.
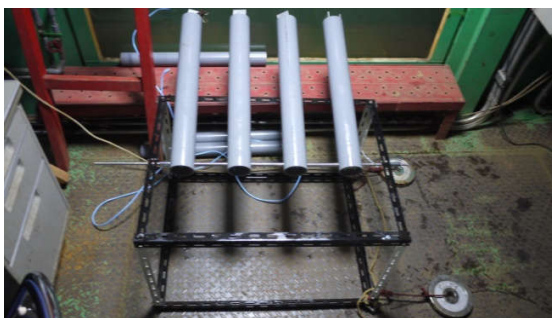
Photograph 1. Cylinder model test setup.
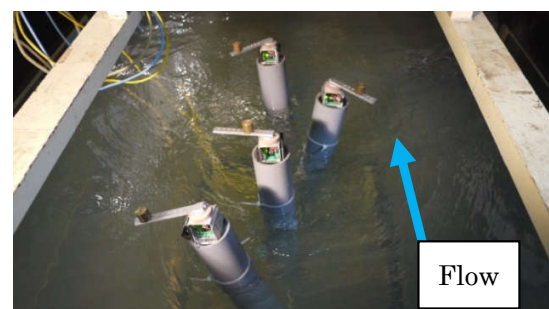
Photograph 2. Test setup with model in circular water channel.

Photograph 3. Hoop generator and sensor. The amplified generator and gravitational acceleration outputs were transmitted via a LAN cable.

Photograph 4. Newly developed PIC18F2523-based data logger system. This system can achieve 8CH 12-bit A/D conversion at a sampling rate of 20 Hz. Measured data are transmitted to a PC via RS232C communication.

Table 1. Test conditions

Weight length [mm]	Velocity [m/s]	Flow angle [deg.]	Cylinder gap [mm]
100	0.25	0°	100
80	0.3	30°	
60	0.35		
40			
without			

Table 2. Generated power

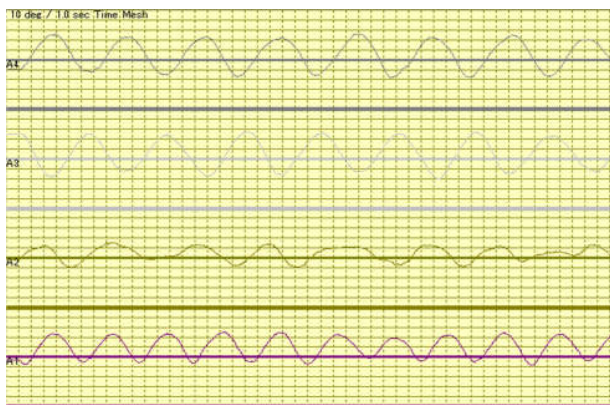| Flow angle 0°		Flow angle 30°	
Vel.[m/s]	Mean[mw]	Vel.[m/s]	Mean[mw]
0.25	0.92	0.25	0.93
0.3	1.16	0.3	1.69
0.35	1.76	0.35	2.02

（Diameter 76mmcylinder）

Figure 3. Sample of rolling motion records (horizontal mesh spacing: 10°).
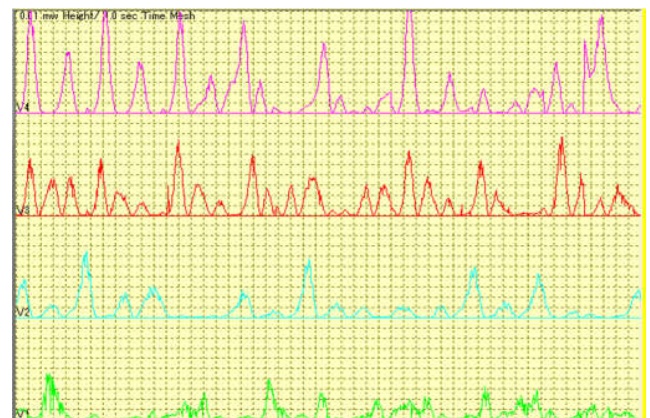

Figure 4. Sample of measured generated power records (horizontal mesh spacing: 0.01 W).

Table 1 lists the experimental conditions of the water tank test, in which two flow attack angles, 0° and 30°, were tested. Figs. 3 and 4 show the rolling motion and measured generated power of each cylinder, respectively, with a flow attack angle of 30°, a tank flow speed of 0.3 m/s, and no weight.

In this system, steady hoop motion and a high energy gain were expected, but the motion of the hoop in the experiment was oscillatory. Table 2 gives the measured generated power, which was rather low because of the oscillatory motion of the hoop. Fig.4 shows that the frequency of the generated energy was higher than that of the hoop motion. This is because the hoop motion is not cyclic but oscillatory.

In this system, the hoop motion should be steady and cyclic, and the generated energy should be higher. To know the hoop motion under many different conditions, an equation of the hoop motion was constructed, as discussed in Section 3. Numerical analysis was then performed, as described in Section 4, allowing the optimal hoop control method and conditions to be found.

3. EQUATION OF HOOP MOTION

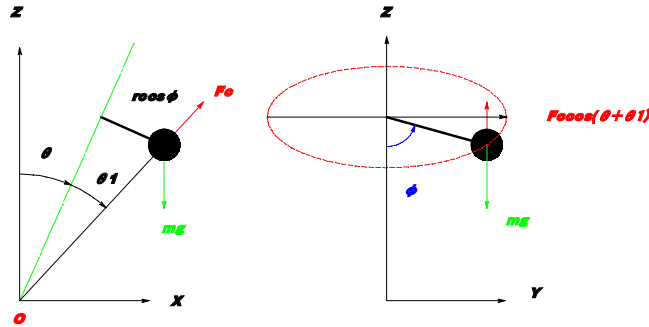The variables describing the hoop weight motion and the coordinate axes used in this study are shown in Fig. 5 and 6.

Figure 5. Definition of axes and forces acting on weight.   Figure 6. Circular motion of weight.

The *y*-axis is the roll axis.

The equation of motion for the weight shown in Fig.5 and 6 is given as

$$mr\ddot{\varphi} + cr\dot{\varphi} + sin\varphi(mgsin\theta + F_c sin\theta) = 0 \qquad (1)$$

The apparent centrifugal force F_c is defined as

$$F_c = \frac{mv^2}{R_1} = \frac{m(R_1\dot{\varphi})^2}{R_1} = mR_1\dot{\varphi}^2 \qquad (2)$$

The geometrical constraint on the angles is

$$sin\theta_1 = \frac{r_1}{R_1} = \frac{rcos\varphi}{R_1} \qquad (3)$$

By substituting equations (2) and (3) into equation (1), the equation of motion can be transformed into

$$mr\ddot{\varphi} + cr\dot{\varphi} + msin\varphi(gsin\theta + r\dot{\theta}^2cos\varphi) = 0 \qquad (4)$$

In this way, R_1 has been eliminated from all terms. Equation (4) can be simplified by making the angular acceleration coefficient equal 1, as

$$\ddot{\varphi} + \frac{c}{m}\dot{\varphi} + sin\varphi\left(\frac{g}{r}sin\theta + \dot{\theta}^2cos\varphi\right) = 0 \qquad (5)$$

The solution to equation (5) describes the motion of the system. However, the more common form of the equation of motion includes the term describing the excitation force on the right-hand side of the equation, as

$$\ddot{\varphi} + \frac{c}{m}\dot{\varphi} + sin\varphi \frac{g}{r} sin\theta = -\dot{\theta}^2 cos\varphi sin\varphi \tag{6}$$

Defining $C = c/m$, $K = (g/r)sin\theta$, and $F_\theta = -\dot{\theta}^2 cos\varphi sin\varphi$ yields

$$\ddot{\varphi} + c\dot{\varphi} + K sin\varphi = F_\theta \tag{7}$$

The obtained equation of motion for the hoop describes nonlinear large-amplitude pendulum motion, and the difficulty of solving it mainly arises from the strong nonlinear external force. Based on this equation of motion, it is possible that the hoop motion will be chaotic. This equation was solved using the numerical Newmark-beta method under the steady constant-amplitude rolling motion of the cylinder. An analysis program was developed in Visual Basic 2010, including a graphical user interface (GUI) to allow the visualization of the hoop motion and generated power.

4 .NUMERICAL ANALYSIS

The numerical analysis conducted in this study considered a simple oscillating sinusoidal form for the external force, which yielded various types of oscillatory hoop motions, as shown in Figs. 7–10. The phase plane diagrams of the hoop motion in Figs. 7–10 are shown in Figs. 11–14, respectively. The motion shown in Fig.7 demonstrated steady and continuous hoop rotation, which is divergent hoop motion. This case had the highest energy generation. This phase of the hoop motion has the divergent tendency, as shown in Fig.11, and represents the chaotic motion. The hoop motion shown in Fig.7 appears to be a steady rotating motion. If the damping force is increased while maintaining steady rotation, the energy absorption from the system increases.

Figs 11–14 show the phase plane diagrams of the hoop motion shown in Figs 7–10, respectively. Fig. 11 shows the chaos divergent condition and corresponds to Fig.7. In Fig.12, which corresponds to Fig.8, a stable trajectory was not found. Conversely, Figs 13 and 14, which correspond to Figs 9 and 10, respectively, show hoop motions that appear to have achieved steady oscillation. In this motion, the phase trajectory stabilized after some oscillation; this type of stability is called Lyapunov stability.

In Table 3, the numerical results of the phase analysis are classified based on the calculation conditions and shows the chaos zone. If the forced oscillation period increases, double-period hoop motion first appears. Further increasing the forced oscillation period causes the chaos divergence zone to appear. Increasing the period beyond this zone destabilizes the hoop motion and causes constant stable oscillation to appear.

Figure 7. Sample of a diverging motion appeared in the hoop weight roll angle. The roll angle is shown from $-\pi$ to π.

Figure 8. Sample of unstable hoop motion. Calculation result is shown in the log period.

Figure 9. Sample of stable motion.

Figure 10. Sample of stable double period motion.

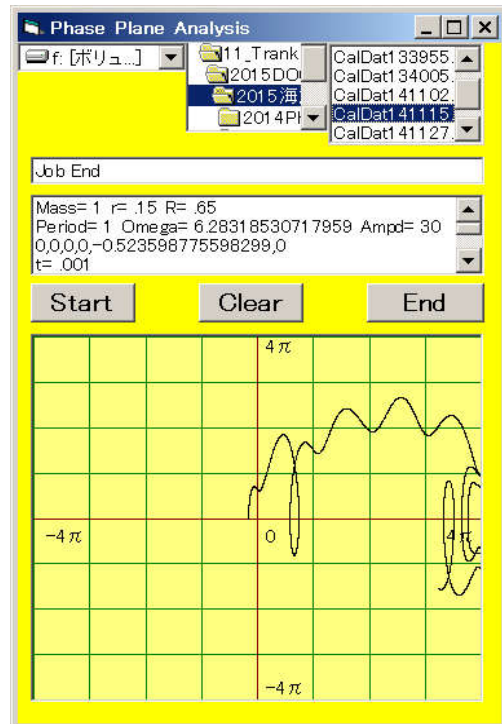Figure 11. Phase plane diagram for motion shown in Figure 7.

Figure 12. Phase plane diagram for motion shown in Figure 8.
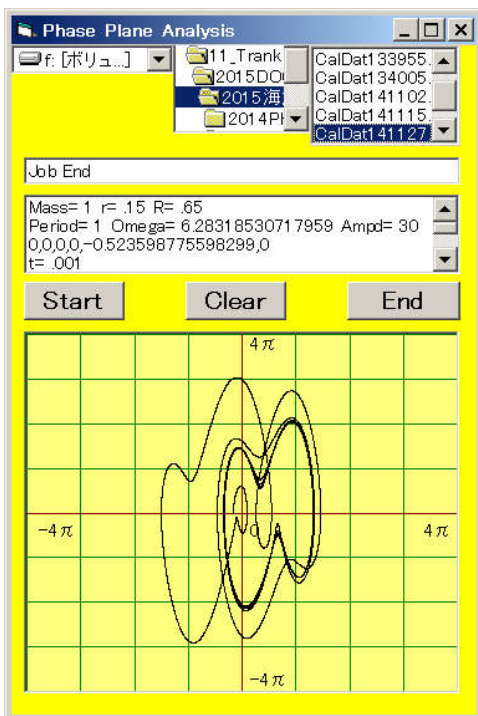

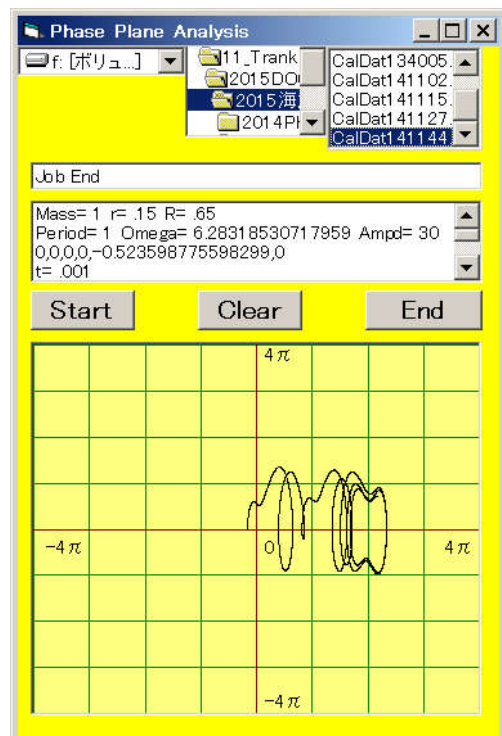Figure 13. Phase plane diagram for motion shown in Figure 9.

Figure 14. Phase plane diagram for motion shown in Figure 10.

Table 3. Categories of calculated double pendulum hoop motion.

Aplitude	10 dg.									
Period(sec)	1		1.5	1.6	1.7			3	4	5
Motion	Without motion	Stable double period	Unstable		Stable diverging				Unstable	Stable

Aplitude	20 deg.									
Period(sec)	0.9	1	1.05	1.5		1.7	2	2.6	3	4
Motion	Without motion	Stable double period	Unstable	Stable diverging			Unstable			Stable

Aplitude	30 deg.										
Period(sec)	0.7	0.8	0.9	1	1.05	1.5		1.7	2	2.6	3
Motion	Without motion	Unstable			Stable diverging			Unstable			Stable

5. EFFICIENCY OF GENERATED POWER

The following two patterns, θ_1 $\theta_{2\,2}$ are considered:

$$\theta_1 = \theta_a sin\omega t \tag{8}$$

$$\theta_2 = \theta_b sin\omega t + n\omega t \tag{9}$$

where θ is the hoop angle and the subscripts 1 and 2 indicate sinusoidal and hoop-type pendulum motion, respectively. Equation (9) describes simple chaotic hoop-type motion. The angular velocities are given by

$$\dot{\theta}_1 = \theta_a \omega cos\omega t \tag{10}$$

$$\dot{\theta}_2 = \theta_b \omega cos\omega t + nt \tag{11}$$

The generated voltage is proportional to these angular velocities, as

$$V_1 = C\theta_a \omega cos\omega t \tag{12}$$

$$V_2 = C(\theta_b \omega cos\omega t + nt) \tag{13}$$

and the electric power W is defined as

$$W = \frac{V^2}{R} \tag{14}$$

The power averaged over one period is

$$E = \frac{1}{T}\int_0^T W dt \tag{15}$$

If we assume that the amplitudes of the angular velocities are the same, i.e.,

$$\theta_a = \theta_b \tag{16}$$

then the energies generated by the pendulum-type and chaotic motions are given respectively by

$$E_1 = \frac{1}{2}(C\theta_a \omega)^2 \tag{17}$$

$$E_2 = \frac{1}{2}(C\theta_a \omega)^2 + (Cn\omega)^2 \tag{18}$$

Equations (17) and (18) can be used to find the absorption energy difference ΔE caused by the difference between the two types of motion, as

$$\Delta E \equiv E_2 - E_1 \tag{19}$$

$$= (Cn\omega)^2 > 0 \tag{20}$$

where C is the damping coefficient, n is the rotation number, and ω is the steady rotation frequency at the divergence point. Equation (20) demonstrates how energy absorption can be increased. Increasing the damping coefficient increases the absorption energy until the motion is no longer chaotic, and constant rotations also increase the absorption energy. This is called the rotation bias effect.

6. CONCLUSION

1. A new type of VIM pendulum with a hoop generator was proposed in this paper. A circular tank test was conducted on a small model of the system to determine its performance. A newly designed data logger was used to obtain the cylinder VIM motion in a flow and the hoop generating power. However, the system performance proved low because the hoop did not achieve a steady turning motion.

2. To theoretically determine the system performance, a new equation of motion for the hoop was developed, and the motion of the hoop was numerically simulated. In the simulated results of the hoop motion, chaotic motion occurred under various conditions because of the large oscillation of the double pendulum. If this chaos phenomenon will be controlled, steady rotation of the generator motor can be easily achieved and leading to higher power generating performance. However, the chaos phenomenon cannot be confirmed by conducting water tank tests. This problem will be addressed in future work.

REFERENCES

1）Shinji Hiejima, Keito Oka, Kenichi Hayashi and Hiroo Inoue : Fundamental experiment for tidal current power generation using flow-induced vibration; The First Flatter Control and it's application, Sept.,(2011), 4-1.pdf, pp88-93

2）J. H. Lee,　M. M. Rernitsas: High-damping, high-Reynolds VIV tests for energy harnessing using the VIVACE converter, Ocean　Engineering 38, (2011) 1697-1712

3）Yutaka Yoshitake, Katsuya yamakami, Akizumi Fukushima: Various Motions of Hula-Hoop and Utilization as Vibration Quenching, JSME,No.98-8,1998.8.17～20,Sapporo,Japan